GMR
The Original

Triazophos Bioaccumulation in Rat Brain: Association with Blood–Brain Barrier Transporter Dysregulation and Oxidative Stress

Smita Jain[1]*, Soumi Sadhu[1], Satyawada Rama Rao[2], Rafat S Ahmed[3,4], Basu Dev Banerjee[3,5], Vinod Kumar Arora[6,7,] Alok Kumar Ravi[8]

[1]Department of Life Science, Sharda School of Bioscience and Technology, Sharda University, Greater Noida, U.P. 201310, India
[2]Superannuated faculty, Department of Molecular Biology, Central University of Andhra Pradesh, Ananthapuramu, Andhra Pradesh, 517704, India
[3]Ex-Professor, Department of Biochemistry, University College of Medical Sciences (University of Delhi) & Guru Teg Bahadur Hospital, Dilshad Garden, Delhi 110095, India
[4]Professor, Department of Biochemistry, Al-Falah School of Medical sciences and Research, Dhauj, Faridabad, Haryana
[5]Distinguished Professor, Adjunct Research Professor Biochemistry, Central Research Facilities Santosh Deem University, Ghaziabad (UP)
[6]Ex-Professor, Histopathology Laboratory, Department of Pathology, University College of Medical Sciences (University of Delhi) & Guru Teg Bahadur Hospital, Dilshad Garden, Delhi 110095, India
[7]Distinguished Professor, Department of Pathology, Hindu Rao Hospital, Delhi 110007, India
[8]Professor, Department of Ocular Biochemistry, R.P.Centre for Opthalmic Sciences, All India Institute of Medical Sciences, New Delhi-110027, India

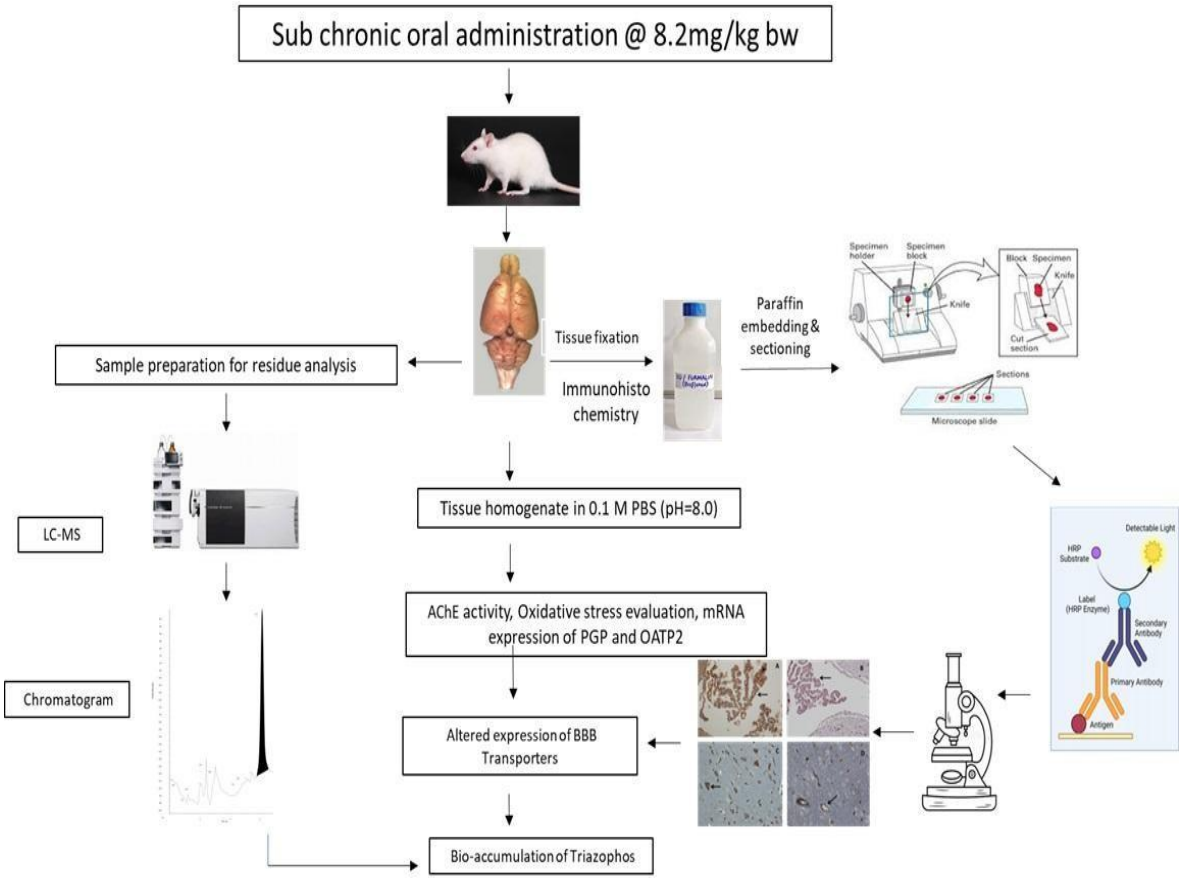
*****_Corresponding author:_ Dr Smita Jain, Email: smita.jain@sharda.ac.in

ABSTRACT
Triazophos (TZ), a broad-spectrum organophosphate pesticide that inhibits acetylcholinesterase enzyme (AChE), is highly toxic to nontarget species through contaminated water and food. In the present study, male Wistar rats were exposed to 8.2 mg/kg TZ (1/10th of oral LD_{50}) for 30 days, and brain tissues were assessed for (a) the gene expression of membrane transporters of blood–brain barrier (BBB) viz., organic anion transporter protein (OATP2) and P-glycoprotein (PGP) via real-time PCR and immunohistochemistry (IHC), (b) oxidative damage and (c) subsequent bioaccumulation in blood and brain tissues via LC–MS, respectively. Results of the present study revealed that compared with those in the control group, PGP expression was reduced, and OATP2 expression was increased ($p<0.001$) in the TZ group. The real-time PCR results were validated by IHC, which revealed moderate to mild PGP staining and moderate to severe OATP2 staining in the TZ-treated rats. Additionally, GSH levels were significantly decreased and lipid peroxidation was increased in TZ treated rats as compared to untreated control. Furthermore, TZ tends to accumulate more ($p<0.01$) in brain tissues than blood in treated rats. These findings suggest that TZ may gain access to the BBB via potential interaction with OATP2, accumulate and induce oxidative stress, which may further contribute a new piece of evidence to the toxicity profile of TZ to reiterate the strict need to monitor the indiscriminate use of TZ in agricultural fields.

Short running title: Neurotoxic effects of Triazophos

KEYWORDS: Pesticides, Neurodegeneration, Triazophos, Blood–brain barrier, P-glycoprotein, Neurotoxicity, Organic anion transporter polypeptide.

GRAPHICAL ABSTRACT



1. INTRODUCTION

Triazophos (TZ), O,O-diethyl O-1-phenyl-1 H-1,2,4-triazol-3-yl phosphorothioate, is a broad-spectrum organophosphorus pesticide (OP) that has been extensively used against a broad spectrum of pests affecting cotton, sugarcane, wheat, maize, potatoes, vegetables, cereals, fruits, coffee and ornamental crops **(Duan et al, 2016**; **Kumari and John, 2019).** The rapid availability of TZ encourages its widespread and unmonitored use as an effective insecticide in agricultural fields across the world. However, such overuse of TZ has a very large detrimental impact on nontargeted entities such as agricultural land, ground water, pesticide applicators and ultimately top consumers because of its long half-life, high chemical stability, photostability and hard-to-degrade mechanism **(Fang et al, 2019)**. The severity of TZ intoxication may vary with dose, route and extent of exposure. Like most OPs, TZs are rapidly degraded and eliminated after a single low-dose exposure, but the rate of elimination decreases to 60% when the exposure is chronic and continuous. TZ adversely impacts primary and secondary consumers by inducing endocrine disruption in pituitary hypothalamic regions, hypertrophy, necrosis and multiorgan toxicity **(Ramesh et al 2024)**.

Like other OPs, the TZ inhibits the enzymatic activity of acetylcholine esterase (AChE), leading to extended depolarization and hyperexcitability at synapses, which results in a cholinergic crisis. Our previous study reported the noncholinergic effects of TZ, such as the induction of oxidative stress and cognitive impairment, due to altered levels of brain-derived neurotrophic factor (BDNF), which is indispensable for the growth, maturation, differentiation and survival of neurons; synaptic plasticity; and memory retention in the hippocampus area of the brain **(Jain et al, 2011)**. Execution of these neurotoxic effects can be better explained if the transport of TZ across the selectively permeable blood–brain barrier (BBB), a monolayer of brain capillary endothelial cells that are fused together by tight junctions and harbor numerous membrane transporters, is known. Among the various membrane transporters located on the BBB, the present study focused on evaluating the gene and protein expression of two transporters, organic anion transporter polypeptide (OATP) and P-glycoprotein (P-GP).

Organic anion transporting polypeptides (OATPs) are a group of influx membrane transporters that are specific to a wide spectrum of substrates, such as xenobiotics (diazinon), thyroid hormones and drugs (digoxin,

opioid receptor agonists, etc.), and exhibit multiple types of tissue localization, including the blood–brain barrier (BBB), choroid plexus, glial cells and neurons in the brain, including the cortex, hippocampus, retina, lung, heart, intestine, kidney, placenta and testis **(Tamai et al, 2000; Schäfer et al 2021)**. It is located on the basolateral (toward the blood) membrane of the BBB and has twelve transmembrane (TM) segments containing a large extracellular domain between TMs 9 and 10, six conserved cysteine residues that resemble the zinc finger domains of DNA-binding proteins in the extracellular loop between TM domains 9 and 10 (**Li TT et al, 2019**). The disulfide-bonded cysteine residues are critical for the proper folding and function of OATPs. In addition, there are N-glycosylation sites in extracellular loops 2 and 5 and the OATP superfamily signature at the border between extracellular loop 3 and TM domain 6. While OATP2 is located primarily on the luminal side, studies have shown that it may also be present on the entire surface of rat brain capillary endothelial cells **(Gao et al, 1999)**. Although OATP may be involved in xenobiotic transport, until recently, there have been no reports on its involvement in the transport of TZ. Given the anti-cholinesterase effect of TZ confirmed by previous research findings, it is imperative to study the expression of OATP2 to understand its putative role in TZ transport to the brain and understand the underlying mechanism of TZ-induced neurotoxicity.

Exploring the inward movement of TZ via membrane transporters embedded in the BBB alone cannot fully explain TZ-induced neurotoxicity; therefore, it is necessary to explore its concomitant or subsequent elimination from highly vulnerable and important body tissue (brain). The present study also evaluated the role of the energy-dependent efflux transporter P-glycoprotein, which is located on the basolateral side. P-glycoprotein (PGP), also known as permeability-glycoprotein or multidrug resistance protein 1 (MDR1), belongs to the ABC transporter superfamily and is encoded by the *MDR1/ABCB1* gene in humans **(Schinkel et al 1999)**. It contributes to the elimination of a wide range of structurally unrelated compounds, including xenobiotics and drugs, from the brain **(Gao et al. 1999; Lee et al. 2001)**, thereby preventing the bioaccumulation of toxic substances inside the underlying tissue, such as the brain. It is specifically localized on the basolateral membrane (toward the blood) in the BBB. In humans, there are two P-GP isoforms: MDR1 and MDR3. However, only the coding product of the *MDR1/ABCB1* gene actively and significantly participates in the disposition of xenobiotics in various organs. However, there are no reports to date regarding its involvement in TZ transport across the BBB. Hence, the present study was designed to define the nature of the interaction between TZ and BBB transporters during the course of action of TZ and identify the mechanism by which it possibly gains entry into the brain. Moreover, this study is the first to estimate the residual concentration of TZ in blood and brain tissues following chronic exposure and helps in understanding the relationship between the extent of exposure and the intensity of damage. In this way, the present study may also help to explore and identify the noncholinergic targets of the TZ, which remain understudied to date.

2. MATERIALS AND METHODS

2.1 Chemicals and reagents

Triazophos (TZ; O, O-diethyl O-(1-phenyl-1,2,4-triazole-3-group) thiophosphate, CAS Registry No. 24017-47-8) was purchased from M/S Hindustan Insecticide Limited (Delhi, India). Primary and secondary antibodies (CytoscanTM HRP detection system) were purchased from Santa Cruz Biotechnology, Inc., USA. All solvents, such as hexane, acetone, isopropanol, chloroform, absolute alcohol, mass-grade formic acid, acetonitrile (ACN) and ammonium acetate, were of HPLC grade purity and were purchased from Merck Biosciences (Germany). Diethyl pyrocarbonate (DEPC), TRIzol and homatropine were procured from Sigma Aldrich (St. Louis, MO, USA), whereas the DNase I kit and RNase Zap were purchased from AmbionTM. Low-melting agarose, a high-molecular-weight DNA ladder (100 bp), and ethidium bromide were purchased from Fermentas (Thermo Scientific, USA). The purified water was collected via a Milli-Q purification system. All other reagents used were of the highest analytical grade and were obtained from Merck Biosciences (Germany).

2.2 Animals and treatment

Wistar male albino rats (150–200 g) were placed in polypropylene cages (17 inch × 11 inch × 6 inch) 5 days prior to the start of the experiment for acclimatization and were fed a nutritionally adequate standard laboratory diet obtained from M/S Hindustan Lever Ltd., Mumbai, India. The animals were kept under standard laboratory conditions at ambient temperature (25 ± 20°C) with a light/dark cycle of 12 h each. Food and water were provided ad libitum. The animals were randomly divided into 2 experimental groups (n = 10 per group). One group was orally administered 8.2 mg/kg body weight (bw) TZ dissolved in olive oil (vehicle) for 30 days. The dose represented 1/10th of the oral LD_{50} of TZ and was selected on the basis of

previously conducted studies in rats **(Jain et al., 2010 and 2011)** as per the existing regulatory toxicity guidelines approved by the Organization for Economic Cooperation and Development (OECD) for chronic toxicity using animal models **(OECD, 2007)**. The other group was administered only vehicle (olive oil) for the same duration and under the same laboratory conditions.
Food consumption, general animal conditions and any other symptoms were observed daily, whereas body weight was recorded weekly. The research protocol used in the present study was approved by the Institutional Animal Ethics Committee, University College of Medical Sciences (University of Delhi) and Guru Teg Bahadur Hospital, Delhi vide approval number UCMS/IAEC/CAH/2011/373 (copy enclosed as supplementary material), and is part of the doctoral thesis of the corresponding author. The care of the animals was carried out as per the guidelines of the Committee for the Purpose of Control and Supervision of Experiments on Animals (CPCSEA), India.

2.3 Sample collection
After exposure, all the rats were fasted overnight. The animals were anesthetized with halothane and decapitated, and blood samples were collected from all the rats in heparinized vials by puncturing the retero-orbital vein. The collected blood was processed within 24 hrs for TZ residue evaluation. The brain tissues were immediately excised, and the hippocampi were isolated. The isolated hippocampi were washed with ice-cold saline, weighed and homogenized at 4°C via a motor-driven Teflon Potter homogenizer. The homogenization buffer contained 50 mM sodium phosphate buffer (pH 7.4) with 50 mM Tris hydrochloride and 1.15% potassium chloride. The homogenate was centrifuged at 7000xg for 15 min at 40°C, and the supernatant was used for assessment of acetylcholine esterase (AChE), reduced glutathione (GSH), and lipid peroxidation (LPO). All the assessments were performed on the same day that the tissue samples were collected. The excised brain tissues were separately processed for analysis of OATP2 and PGP mRNA expression and protein expression via immunohistochemistry, the details of which are described in the methodology section below.

2.4 Acetylcholine esterase (AChE) activity
Brain AChE activity was measured by adding 20 µl of substrate (0.075 M acetylthiocholine iodide) and 400 µl of brain tissue homogenate to 100 µl of 0.01 M 5,5'-dithiobis-2-nitrobenzoic acid (DTNB) in 0.1 M phosphate buffer (pH=7.0) as described previously by **Ellman et al. (1961).** All the reagents were freshly prepared before every set of experiments. There was a 5-min preincubation period, and the reaction was conducted at 37°C. The specific activity of AChE was measured at 412 nm at intervals of 60 s for a period of 5 min. The molar extinction coefficient of the yellow color adducts formed between DTNB and thiocholine was 13600 M-1 cm-1. The total protein content of the tissue homogenate was estimated via the method of **Lowry et al. (1951)**. The results are expressed as micromoles of substrate hydrolyzed per min per gram of protein.

2.5 Reduced glutathione (GSH)
The GSH content was evaluated by adding 5% trichloroacetic acid to the tissue homogenate supernatant followed by centrifugation at 5000 rpm for 15 min at 4°C. This step aids in the precipitation of the total proteins. The resulting supernatant was added to the assay mixture containing 0.3 M sodium phosphate (pH 8.4) and 0.4% w/v DTNB in 1% trisodium citrate. After thorough mixing, the absorbance of the mixture was immediately measured at 412 nm. The results are expressed as µg/g wet tissue **(Elman et al, 1959)**.

2.6 Lipid peroxidation (LPO)
The extent of LPO in brain tissue was assayed by measuring malondialdehyde (MDA) levels via the method described previously by **Ohkawa et al. (1979)**. The formation of the MDA-TBA adduct was measured at 532 nm following extraction with butanol: pyridine (15:1 v/v), and the results are expressed as µmoles/g wet tissue.

2.7 mRNA expression by real-time PCR
2.7.1 RNA extraction and cDNA synthesis
The brain tissues, especially the hippocampi, were excised, washed immediately with ice-cold saline and processed the same day for RNA isolation. Briefly, 100 mg of RNA was isolated via the TRIzol method

according to the manufacturer's instructions. In short, a Teflon-Potter homogenizer (Remi, India) was used to homogenize 100 mg of tissue in 1 ml of TRIzol re agent, and the tissue was centrifuged at 12000 x g for 10 minutes at 40°C. After the supernatant was collected in a new tube, 0.2 ml of chloroform was added. The mixture was vortexed and centrifuged at 12000 × g for 15 min at 40°C, and the RNA- containing upper aqueous phase was collected in a new tube. After being combined with 0.5 ml ofisopropanol for 10 to 15 min at room temperature, the obtained RNA solution was centrifuged at 12000 x g for 10 minutes at 40°C. The resulting RNA pellet was subsequently washed with 75% ethanol twice at 7500 × g at 40°C. The pellet was subsequently air dried and resuspended in 50 µl of nuclease-free water. The isolated RNA samples were treated with DNase I before their respective purity and concentration were measured at 260 nm with a NanoDropTM. A first-strand cDNA synthesis kit for RT–qPCR (Thermo Scientific, USA) was used (within 8 hours of isolation) for cDNA synthesis.

2.7.2 Quantitative real-time PCR

The Rotor gene Q, Qiagen, was used for real-time PCR, with a final volume of 20 µl per tube. The reaction mixture included 3 µl of cDNA from the RT mixture, 0.5 µM primer, 2 µl of fluorescent Syto 09 dye diluted 1:100, and 10 µl of Pyrostart Fast PCR mix. The primers designed via PRIMER BLAST are detailed in Table 1. The PCR conditions are listed in Table 2. The fluorescence level at which Syto 09 was released was measured at the end of each cycle. At the end of each cycle, the fluorescence emitted by Syto 09 was measured. The samples were subjected to a temperature ramp (from 70°C to 95°C, 2°C/s) with continuous fluorescence monitoring for melting curve analysis at the end. For each PCR product, a single narrow peak was obtained by melting curve analysis at a specific temperature. Each sample was assayed in duplicate, and the analysis was performed with relative quantification software provided with the system. The no-template control (NT) was also included in each experimental run. The reliability and reproducibility of the amplification of target genes were reverified by using another gene, i.e., 18S rRNA, as an internal control. Owing to the nonavailability of any significant difference in the relative quantification of the target gene with respect to each internal control at several runs, only one internal control, i.e., β-actin, was considered for the final calculation of the relative quantification of target gene(s) in all the samples. Moreover, the amplification specificity was further confirmed by subjecting the PCR products from each primer pair to agarose gel electrophoresis. All reagents were procured from Fermentas and Thermo Scientific, USA.

The change in Ct (ΔCt) was calculated for all the samples, each of which was run in triplicate, by subtracting the average Ct of the reference gene from that of the target gene. The relative quantification was performed via the 2-ΔΔCt method as described previously **(Livak and Schimittgen, 2001)**.

Table:1 Primer sequence for Target and Internal control genes

Gene	Primer sequence	Amplicon size (bp)	Reference
PGP	5' AAGGATCAGGAACAATAAA 3' (Reverse) 5'GATGGAATTGATAATGTGGACA3' (Forward)	351	Zhang et al, 1996
OATP2	5'AACATGCTGGTTGAAAATGAAGG3' (Reverse) 5'GTACTCAAGATTTTCCCAGGGAAA3' (Forward)	84	Wang et al, 2003
β-actin	5' CGGATGTCAACGTCACACTT 3' (Reverse) 5' GGGAAATCGTGCGTGACATT 3' (Forward)	253	Musazzi et al, 2009
18s rRNA	5' CGCTCCGAGGGCCTAACTA 3' (Reverse) 5' TTGATTAAGTCCCTGCCCTTTGT 3' (Forward)	77	Wang et al, 2009

Table 2: Temperature conditions for Real Time PCR

S.No	Steps	Temperature	Time	No. of cycles
1.	Initial denaturation	95 °C	1 min	1
2.	Denaturation	95 °C	**2 sec**	40
3.	Annealing	53 °C	**5 sec**	
4.	Elongation	72 °C	**5 sec**	
5.	Final Extension/ Gain optimization	75 °C	1 min	1

2.8 Immunohistochemistry analysis

The hippocampi were isolated from the rat brain, washed immediately with ice-cold saline and fixed in 10% neutral buffered formalin for 24–48 h. Five-micron-thick paraffin-embedded sections were cut on polylysine-coated slides and analyzed for protein expression via immunohistochemistry. Briefly, the slides were dewaxed in xylene followed by rehydration in graded alcohols ranging from 100% to 70%. Then, antigen retrieval was carried out in citrate buffer (pH=6) at 95°C for 15 min by using an EZ Retriever system (Biogenex Laboratories, India). The slides were then allowed to cool at room temperature in citrate buffer. Then, the endogenous peroxidases were blocked by the addition of 4% hydrogen peroxide in methanol (v/v), and the slides were incubated in the dark for 1 h at room temperature. After being washed with Tris-buffered saline (TBS) (pH=7.4), the slides were incubated with 3% skim milk in TBS (w/v) at room temperature for 1 h. Then, anti-rat P-GP and anti-rat OATP2 primary antibodies (Santa Cruz Biotechnology, Inc.) were added at 1:20 and 1:50 dilutions, respectively. The slides were incubated at room temperature for 2.5 h. Afterwards, the slides were washed with TBSTx [TBS containing 0.02% Tween 40 (v/v)] to remove the unbound primary antibodies. The addition of an HRP detection system containing streptavidin and biotin and incubation for 1 h at room temperature further amplified the signal specificity. The unbound antibody was removed by washing thoroughly with TBST, followed by the addition of an HRP substrate, i.e., 3,3'-diaminobenzidine (DAB), and subsequent incubation in the dark for 5–10 min at room temperature. The slides were counterstained with hemotoxylin followed by rinsing with water to remove excessive stain. Then, the slides were dehydrated in graded alcohol ranging from 70% to 100%, followed by a final rinse with xylene. The slides were mounted in DPX.

2.9 Pesticide residue analysis in the blood and brain

2.9.1 Calibration standard

A stock solution of TZ (1 mg/ml) was prepared in pure acetonitrile (ACN). A calibration standard was prepared in 50% methanol at concentrations of 15.62, 31.25, 62.5, 125, 250 and 500 ng/ml. A stock solution (1 mg/ml) of internal standard (IS) was prepared by dissolving homatropine in methanol. It was further diluted in extraction solvent, which consisted of 70% ACN containing 0.1% formic acid and 30% water containing 2 mM ascorbic acid up to 100 ng/ml. TZ was further spiked in whole blood and plasma at concentrations of 15.62, 31.25, 62.5, 125, 250 and 500 ng/ml.

2.9.2 Whole blood and brain tissue sample preparation

Blood samples (20 µl) were mixed with 200 µl of extraction solvent. Then, the mixture was vortexed for 2 min and centrifuged at 7000 × g for 10 min. The supernatant (150 µl) was loaded on a 96-well microplate for final residue analysis. Freshly excised brain tissues (~100 mg) were chopped and mixed with 300 µl extraction solvent. Furthermore, the tissue was homogenized for 2 min and sonicated for 10 min. Finally, it was centrifuged at 7000 × g for 10 min. The supernatant (150 µl) was loaded on a 96-well microplate for final residue analysis.

2.9.3 LC–MS/MS parameters and conditions

Chromatographic separation was achieved via a Thermo Accela UHPLC system with a ZIC-HILIC column (5 µm particles, 20 × 2.1 mm size), a quaternary pump connected to an online degasser, an autosampler and a photodiode array detector (PDA). A 20 µl sample was injected into the UHPLC system with a run time of 7 min. The mobile phase consisted of ACN, containing 0.1% formic acid and water containing 0.1% formic acid, and was pumped at a rate of 0.5 ml/min for 2.5 min, 0.7 ml/min for 3–7 min. The linear gradient program was as follows: 0 min 70% A, 2.5 min 70% A, 3 min 95% A, 5 min 95% A and 7 min 70% A, which was maintained for analytical separation. Chromquest software version 4.1 was used to control all UHPLC parameters.

Tandem mass spectrometric detection of the analyte and internal standard (IS) was carried out on a linear ion trap quadrupole LC–MS/MS mass spectrometer 4000Q TRAP ABSciex instrument equipped with a turbo ion spray (ESI) source operated in positive ion mode. The following MS parameters were set: curtain gas, 20; ion spray voltage, 5.5 kV; ion source temperature, 400°C; ion source gas-1, 40; and ion source gas-2, 60. The differential potential (DP) was set at 97, and the entrance potential (EP) was set at 11. The DP and EP for the internal standard (IS) were set at 30 and 10, respectively. Quantification was performed in single ion monitoring (SIM) mode on the basis of the molecular adduct ion for TZ m/z 314.1. The transition for

homatropine (IS) was m/z 276.1. Data acquisition and integration were performed via Analyst 1.4.2 software equipped with an MS instrument.

2.9.4 Calibration curve, linearity and sensitivity

A calibration curve at three concentrations ranging from 5.62 to 250 ng/ml was derived from the peak area ratio of TZ to IS. The concentration of TZ was calculated from these area ratios via a calibration curve. The linearity of the calibration curve was also calculated, and a correlation coefficient (r2) of 0.99 or better was selected. The r2 for TZ was 0.9997. The lower limit of quantification (LLOQ) was defined as the lowest concentration with a coefficient of variance (%CV) < 20%.

2.10 Statistical analysis

The results are presented as the mean ± S.E.M. For expression studies, transcript levels obtained from real-time PCR measurements were normalized relative to β-actin levels for each sample (average of PGP or OATP-2 triplicates divided by average of β-actin triplicates) and analyzed via an unpaired *t* test. The difference in TZ residue in the blood/brain between the treated groups was analyzed via an unpaired *t* test. Pearson's correlation was used to identify any associations between TZ residues in the blood or brain and gene expression. Differences were considered significant when $p > 0.05$.

3. RESULTS

3.1 AChE activity

AChE activity in brain tissues was significantly ($p<0.001$) lower in the TZ-treated rats than in the control rats (Fig. 1). The results of AChE inhibition are presented as the change in AChE activity per minute per gram of protein in brain tissues.

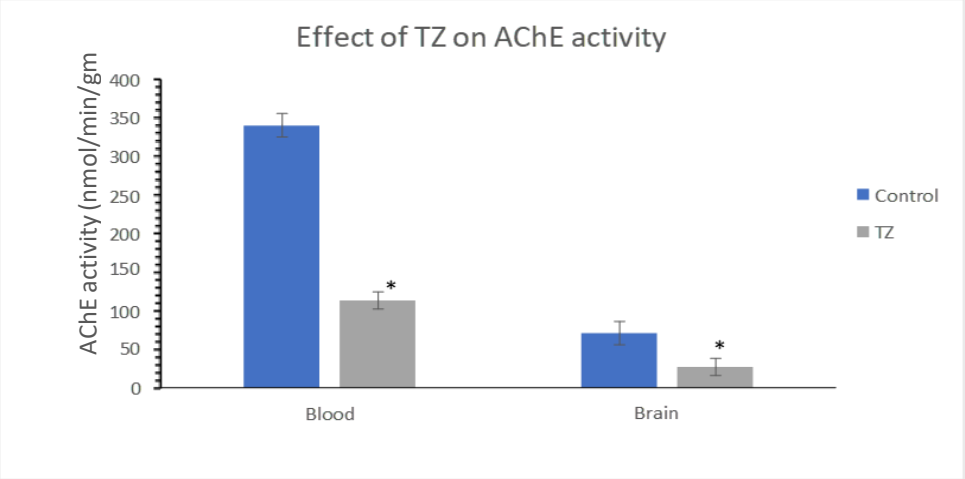


Fig 1: Enzymatic Activity of Acetylcholine esterase in control and TZ treated rats. Significant difference at $p<0.05$.

3.2 Reduced glutathione

A significant ($p<0.001$) decrease in glutathione (GSH) levels was detected in the brain tissues of rats treated with TZ compared with those of control group rats after exposure for 30 days (Fig 2).

3.3 Lipid peroxidation

A significant ($p<0.001$) increase in the brain MDA level was detected in the rats treated with TZ compared with the control rats after exposure for 30 days. The extent of MDA accumulation corresponds to the degree of lipid peroxidation in brain tissue (Fig. 2).

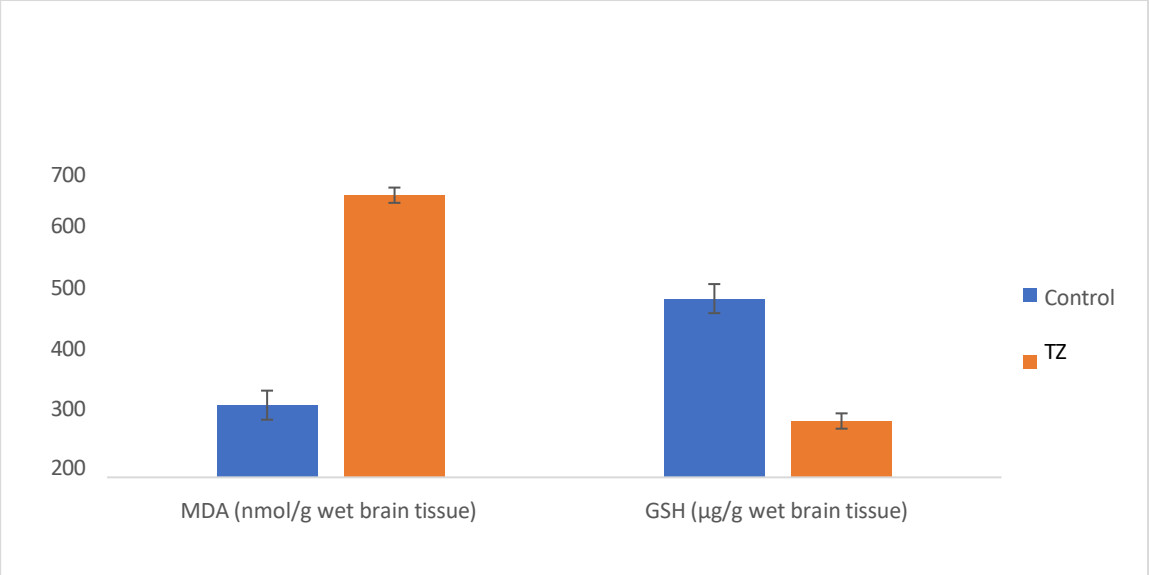


Fig 2: Effect of TZ on the oxidative stress parameters in brain tissues. Significant ($p<0.01$) increase in malondialdehyde levels (MDA; indicator of lipid peroxidation) and concomitant reduction in reduced glutathione (GSH) levels in TZ treated rats as compared to control group rats.

3.4 mRNA expression and protein levels of OATP2 in the rat brain

The relative expression of OATP2, normalized to that of β-actin (internal control), was significantly greater ($p<0.01$) in the TZ-treated rats than in the control rats (Fig 3). These results are in agreement with the findings of **Gao et al. (1999) and Schäfer et al. (2021)** and confirm the localization of OATP2 in only the basolateral membrane of the choroid plexus cells of the BBB and in the basolateral and luminal membranes of endothelial cells and neurons, respectively, as shown in Figure 4. Treatment with TZ for 30 days significantly altered OATP2 expression at both locations. The immunohistochemistry results revealed moderate to severe OATP2 staining in the basolateral membrane of choroid plexus epithelial cells and capillary endothelial cells of the hippocampus in the TZ-treated rats compared with the control group rats (Fig. 4A-D). Additionally, OATP2 expression was severely increased in the hippocampal neurons of the TZ-treated rats compared with those of the untreated control rats (Fig. 4E, F and H). The specificity of OATP2 staining was standardized in normal rat livers as a positive control (Fig. 4G), as it was found to be localized in the sinusoid and bile canalicular membranes of hepatocytes in the midzonal to periportal areas. The significant increase in OATP2 expression was also evident and supported by the results of OATP2 mRNA expression studies via real-time PCR.

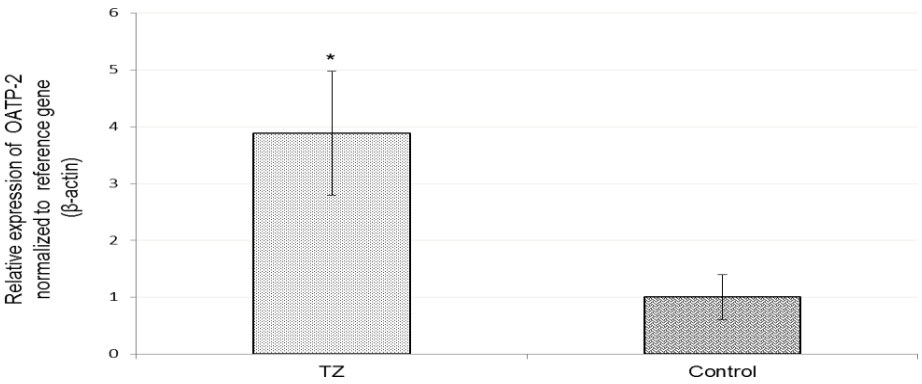


Fig 3: Relative expression of OATP2 in rat brain by Real time PCR. *Significant difference at $p<0.05$.

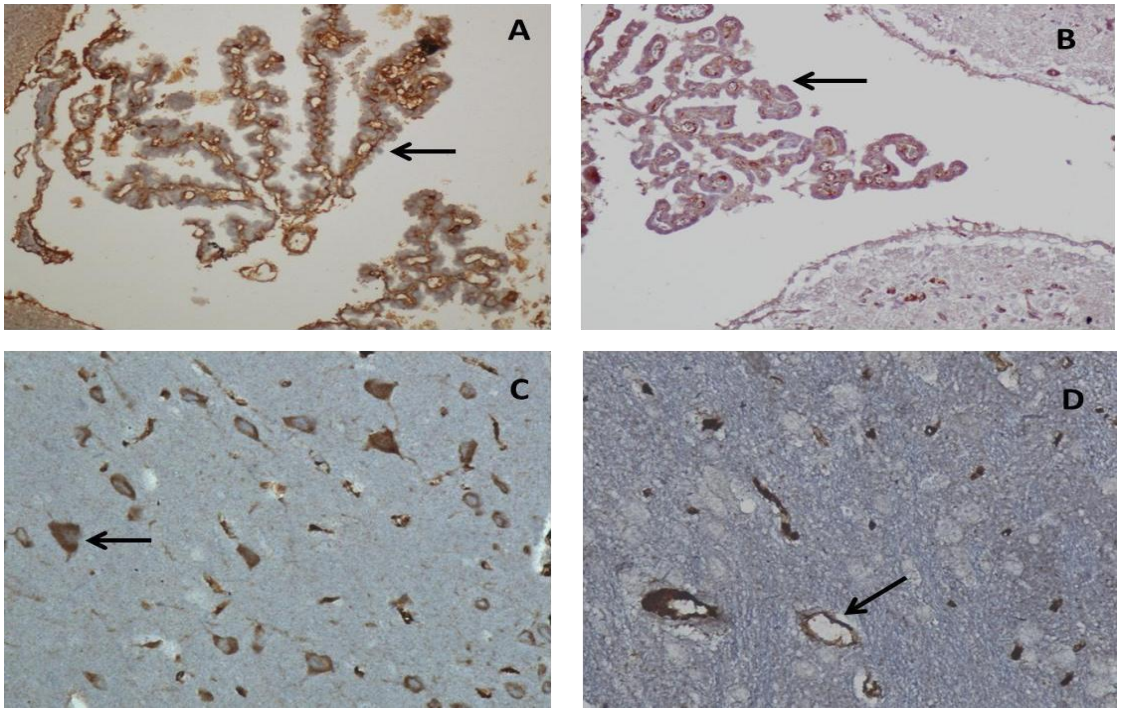


Fig 4: Immunohistochemical localization and expression of OATP2. Intensity of OATP2 specific staining indicating its expression was moderate to severe in basolateral epithelial membrane of choroid plexus in TZ treated group (A) as compared to control group (B). OATP2 localization in brain endothelial capillaries of control group (C) and TZ treated rats (D). OATP2 localization was also observed in hippocampal neurons of control group (E) and TZ treated rats (F, H). Positive control for OATP2 is shown in terms of its localization in bile canalicular membrane (basolateral sinusoidal expression) in midzonal to perivenous hepatocytes but not in the periportal hepatocytes in normal rat liver (G). Magnification A-G (20X); H (40X).

3.5 mRNA expression and protein levels of PGP in the rat brain

The relative mRNA expression of PGP is shown in Figure 5, whereas the IHC results are summarized in Figure 6. The results of the present study revealed that chronic exposure to TZ significantly altered the expression and activity of the efflux pump PGP in the rat brain, as evidenced by the moderate to mild intensity of PGP-specific staining in capillary endothelial cells and choroid plexus epithelial cells of the BBB in the TZ-treated rats compared with the control group (Fig 5A-C). A positive control for validating specific PGP staining was carried out in rat liver tissue, wherein the staining was found in the bile canalicular membrane and around sinusoids (Fig 5D). These findings corroborate the results of the real-time PCR-based mRNA expression studies, which revealed significantly ($p<0.01$) decreased expression of PGP, normalized to that of β-actin (internal control), in the brains of the TZ-treated rats compared with those of the control group rats (Fig 6).

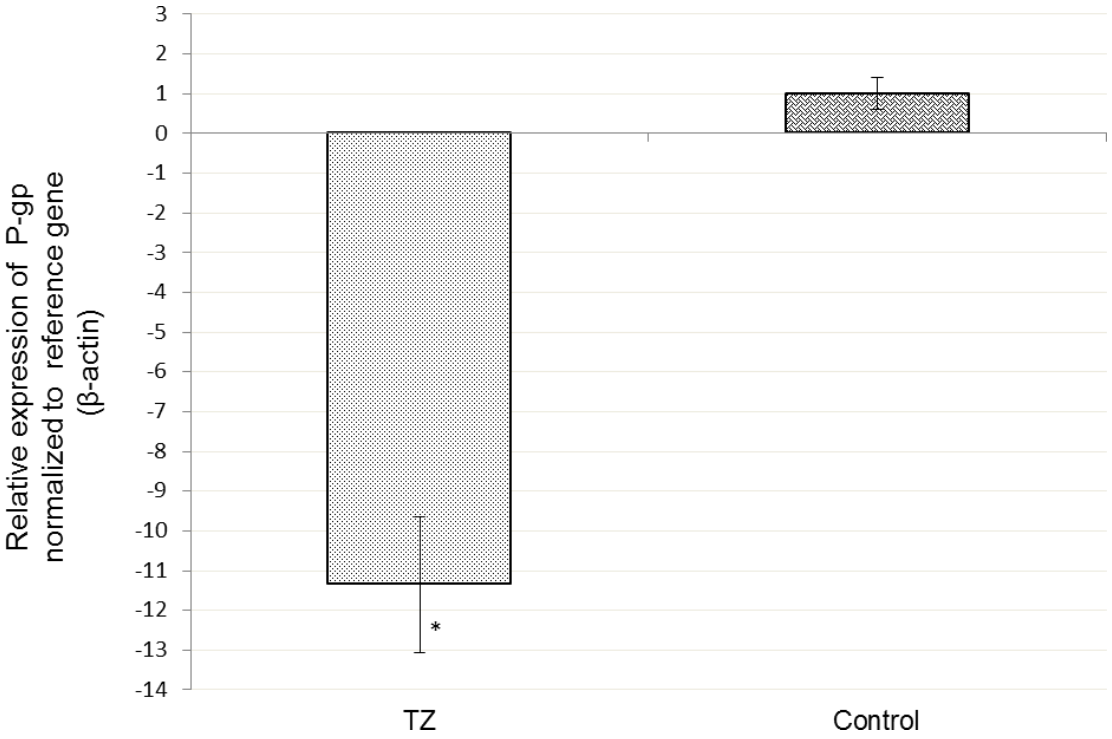


Fig 5: Relative expression of PGP in rat brain by Real time PCR. *Significant difference at p<0.05.

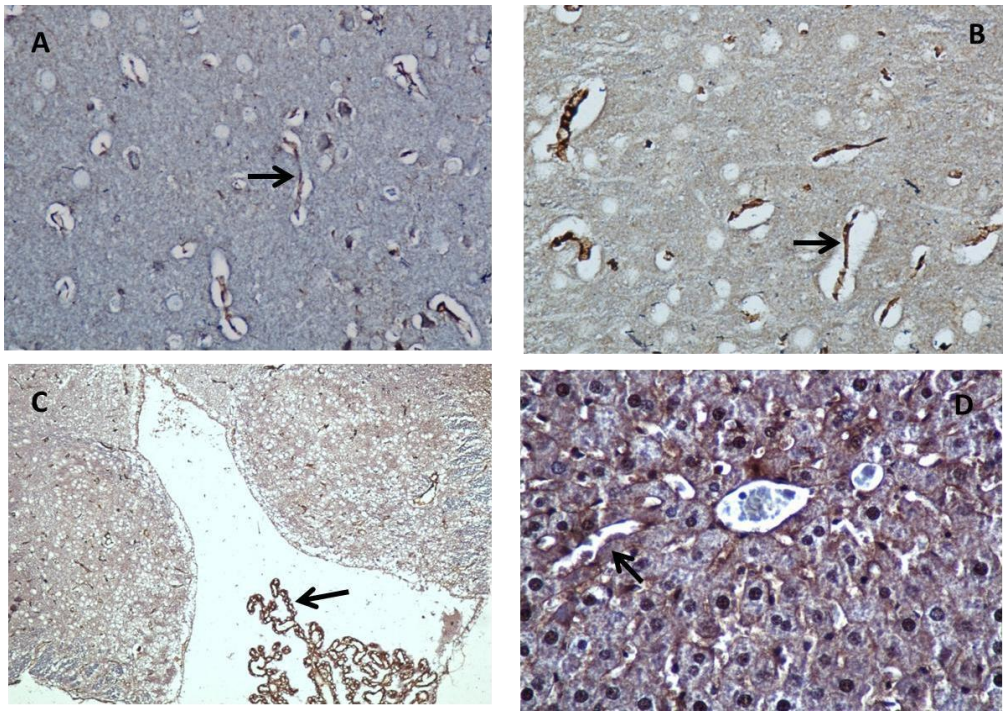


Fig 6: Immunohistochemical localization and expression of PGP. Intensity of PGP specific staining indicating its expression was mild to moderate in brain endothelial cells of TZ treated group (A) as compared to control group (B); choroid plexus staining of PGP in control group (C). PGP staining in control rat liver (as positive control) was evident in the bile canalicular membrane and around sinusoids (D). Magnification 40X (A, B, D) and 20X(C).

3.6 TZ residue analysis in the blood and hippocampus by LC/MS-MS

The TZ residue levels in the blood and brain are presented as the means ± S.E.M.s and are shown in Table 3.

Significantly higher TZ residues ($p<0.000$) were detected in brain tissues than in blood in TZ-treated rats. The concentration of TZ was calculated from the standard calibration curve, in which different known concentrations of TZ were plotted against the area under the curve (Fig. 7). A representative chromatogram for TZ residue analysis via LC–MS/MS is shown in Figure 8. No residues of TZ were found in the blood or brain tissue of the control group rats.

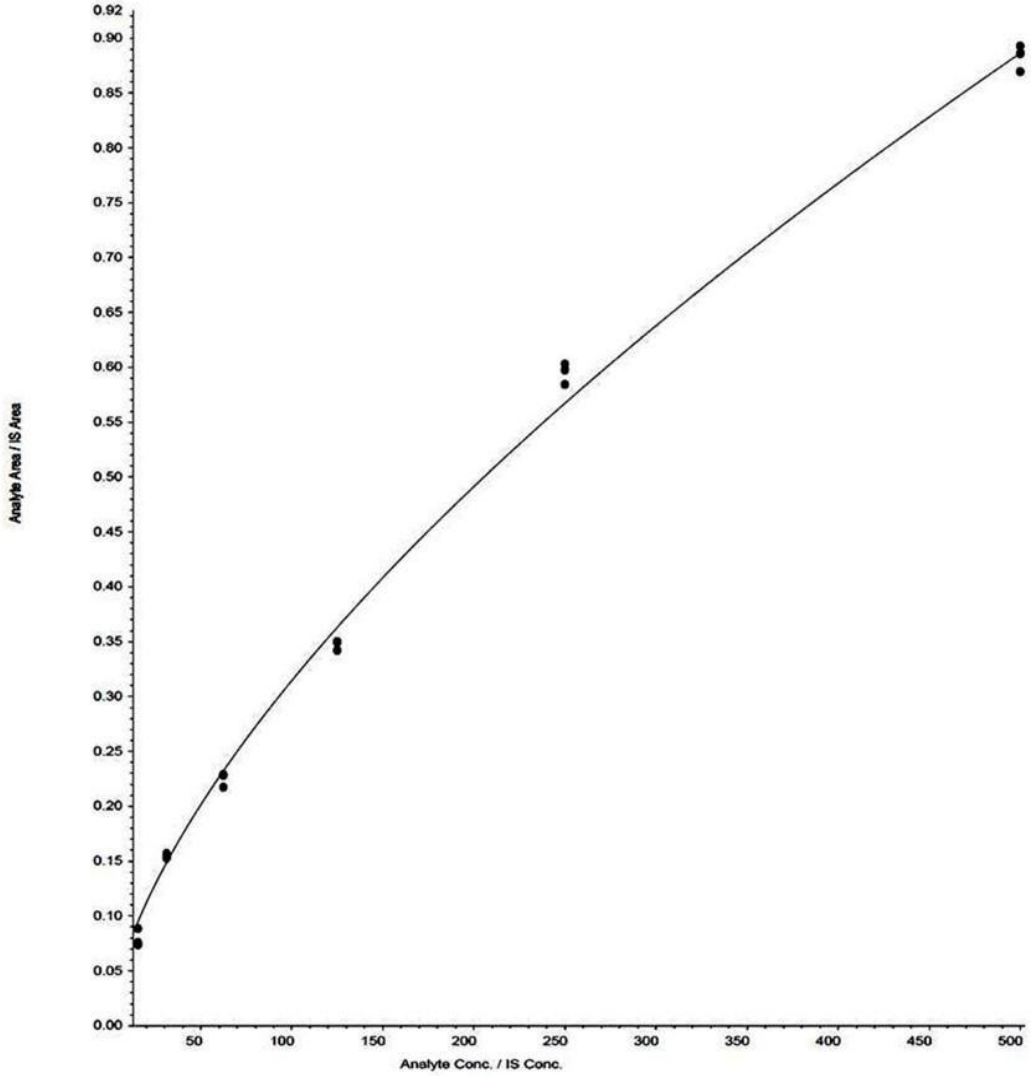


Fig 7: Standard or Calibration curve for Triazophos (TZ) (15.6 – 500ng) estimation by LCMS/MS.

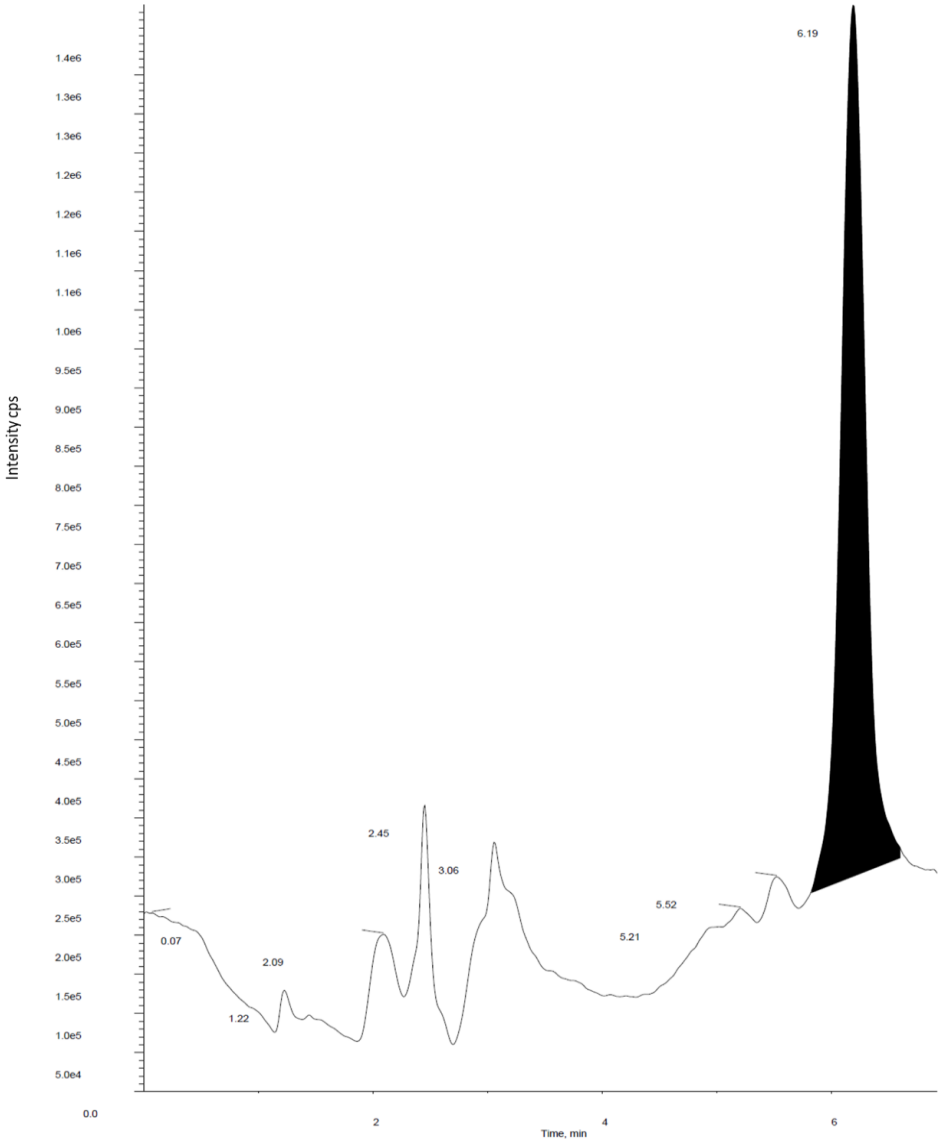


Fig 8: Representative photograph of Triazophos (TZ) estimation by LCMS/MS.

Table 3: TZ residue levels in blood and brain tissue

Group	Sample type	TZ residue (ng/ml) (Mean ± S.D.)	p value	Pearson's correlation coefficient (r) between residue levels in blood and brain
Control	Blood	0	NA	NA
	Brain	0		
TZ treated	Blood	17.233 ± 3.08*	0.00	0.892 ($p<0.001$)
	Brain	3868.33 ± 854.9*	0.00	

NA: Not Applicable

3.7 Pearson's correlation

A significant negative correlation ($r= -0.892$; $p<0.038$) was found between the residual TZ levels in the blood and brain tissues of the TZ-treated rats. Moreover, a significant positive correlation ($r = 0.962$; $p<0.001$) was observed between brain residue levels in the TZ and OATP2 expression, and a significant negative correlation ($r= -0.711$; $p=0.028$) was observed between TZ blood residue levels and OATP2 expression, thus

indicating the involvement of OATP2 in TZ transport from the blood to the brain. Concomitantly, a significant negative correlation (r = - 0.634; p=0.036) was observed between brain residue levels in the TZ and P-GP (efflux pump) expression, and a significant strong positive correlation (r = 0.366; p=0.172) was observed between blood residue levels in the TZ and PGP expression.

4. DISCUSSION

Owing to the indiscriminate use of OPs in agricultural and public health programs worldwide, environmental pollution poses a major threat to human health. However, there is no consensus with respect to the quantitative indices of TZ-induced neurotoxicity except for the inhibition of AChE. The results of the present study also showed that TZ significantly inhibited the enzymatic activity of AChE in brain tissue, which is the primary mechanism of its harmful action. Concomitantly, the present study also attempted to identify a few noncholinergic targets of TZ in the brain, such as the significant increase in lipid peroxidation and the corresponding reduction in reduced glutathione (GSH), which scavenges and antioxidant effects to combat increased oxidative stress following TZ exposure, in the brain tissues of TZ-treated rats. In addition, a compound must gain access across the BBB, a specialized monolayer of endothelial cells connected to each other via tight junctions and harboring numerous xenobiotic transporters on either or both sides of the membrane, to confer any type of neuronal damage. The present study is the first to explore the possible mechanism of TZ transport across the BBB, although the anticholinesterase activity of the latter has long been known. The results of the present study revealed cross-talk between TZs and BBB transporters, thus enabling us to understand the primary pathway through which TZs enter the brain for subsequent neurotoxicity. The present study is also the first to evaluate the residual levels of TZ in the blood and brain following chronic exposure. The results of the present study demonstrated the localization of OATP2 in capillary endothelial cells and basolateral epithelial cells of the choroid plexus in the rat brain (Fig 2-B, D), which is in agreement with earlier findings reported by **Gao et al. (1999)** and **Schäfer et al. (2021).** In addition to their localization, the mRNA expression and protein levels of OATP2 were significantly increased after chronic exposure to TZ (Figs 3 and 4) and were significantly positively correlated with the TZ residues in the brain (Table 3; Figs 7--8). These findings suggest the role of TZ as a potential substrate for OATP2, whose increased expression of OATP2 will gradually be responsible for increased influx of TZ in the brain with respect to the concentration of the latter in blood. This finding also indicates that OATP2 might be involved in the absorption, distribution and transport of TZ. These interpretations are supported by another study that concluded that rat OATP is localized in endothelial cells of the BBB, where it can mediate the uptake of drugs such as opioid peptides **(Hagenbuch and Meier, 2003)**. However, the potential involvement of OATP2 in TZ transport needs further exploration in terms of its subsequent impact on the induction and expression of phase I and phase II metabolic enzymes, which are generally known for xenobiotic detoxification in the brain. TZ is generally metabolized into three metabolites, viz., 1-phenyl-3-hydroxy-(1*H*)-1,2,4-triazole (the main metabolite) and its glucuronide and sulfate conjugates, although their stability varies from one organ to another. Although the excretion of approximately half of the administered dose of TZ occurs within 48 hrs after a single exposure to TZ, the latter decreases if the exposure is prolonged and continuous **(Triazophos Evaluation, 2002)**. Since these metabolites are highly unstable and are readily converted back to the parent compound TZ, they may contribute to the increased bioaccumulation of parent TZ compounds in the brain, which is one of the exclusive findings of the present study (Table 3; Figs. 7--8)**.** This conversion may have contributed to the maintenance of an increased concentration of TZ and subsequent toxicity of TZ in the brain, as shown graphically in Fig 9.

In addition to increased transport of TZ via OATP2, increased TZ residue levels can also be attributed to a reduced rate of elimination of the parent compound and/or its metabolites by xenobiotic efflux transporters such as P-glycoprotein, which mediate the ATP-driven elimination of a broad spectrum of substrates across the BBB. These observations are supported by the results of the present study, which revealed that TZ significantly inhibited the mRNA expression and protein levels of PGP, suggesting that such inhibition occurs at the transcriptional and posttranscriptional levels (Figs. 5, 6). These findings are also in agreement with previous reports indicating that organophosphate pesticides such as phosalone and diazinon, either alone or in combination, are potent inhibitors of PGP *in vitro* as well as in rodent models **(Pivcevic and Zaja 2006)**.

On the other hand, some OPs, such as chlorpyrifos, were found to increase PGP expression in an *in vitro* model system, thereby increasing the efflux of PGP substrates **(Agarwala et al 2004)**. Owing to existing contradictory reports regarding the effects of OPs on PGP function, it is necessary to distinguish each pesticide for its ability to serve as a substrate for or inhibitor of PGP. It has been suggested that PGP

inhibitory pesticides usually execute this inhibition by binding to PGP; however, such binding does not lead to transport **(Bain and LeBlanc 1996, Sreeramulu et al 2007)**. Binding depends on the lipophilicity and molecular mass of the substrate molecule and leads to a conformational change in the PGP structure, which may contribute to the decreased functional activity of PGP at the BBB **(Gottesman et al 2002, Bain et al 1997)**.

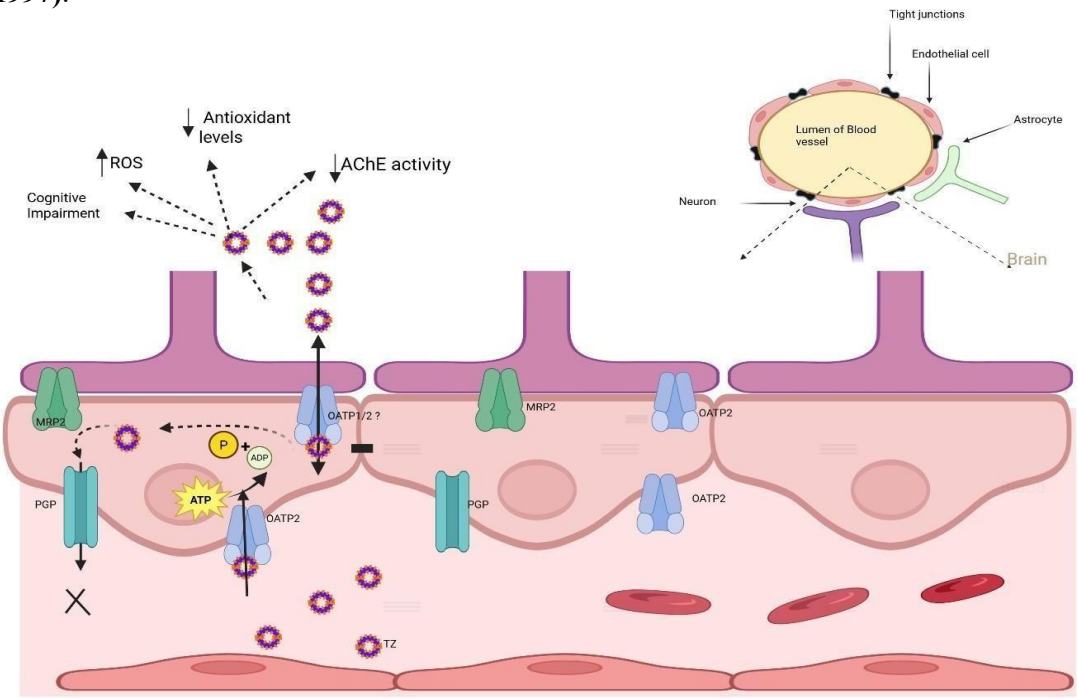


Fig 9: Schematic diagram showing mechanism of TZ entry in to the brain by increasing its influx via OATP2 and decreasing its efflux by P-glycoprotein at BBB. TZ: Triazophos, OATP2: Organic anion transporter polypeptide, P-Gp: P-glycoprotein. Dotted arrows indicate the biological actions of TZ inside brain. Black arrows indicate the direction of transport across BBB. TZ may bind to OATP2 and pumped inside the brain by utilizing the energy released during ATP hydrolysis in BBB. Once TZ enters the brain, it exerts various biological actions via induction of Reactive Oxygen species (ROS), decreasing antioxidant levels thus promoting the onset of oxidative stress, inhibition of acetylcholine esterase (AChE), cognitive impairment in hippocampus. TZ like other xenobiotics are subjected to phase I and phase II detoxification reactions but the resultant metabolites were found to be highly unstable in brain. The possible conversion of these metabolites to parent compound (evident by high residual TZ concentration in brain) may alter the structural integrity of PGP and hence escapes elimination into the blood.

This decrease in PGP expression reflects its compromised ability to remove xenobiotics from the brain, thus increasing the risk of abnormal accumulation of toxic compounds in the brain owing to subsequent neurotoxicity and the development of neurodegenerative diseases (**Bartels et al 2008**). Our results support this statement by showing significantly high bioaccumulation of TZ residue levels in the brain (Table 3; Figs. 7-8) and correspondingly decreased PGP expression at the BBB, indicating that the latter may bind to PGP and cause a conformational change in the BBB transporter structure, which in turn might reduce TZ efflux from the brain. However, the substrate specificity of these two BBB transporters with respect to TZ needs further validation via specific binding assays in living cellular or *in vitro* models, which is an important limitation of our study because of the lack of advanced radioactive laboratories and research facilities at our institute. The results of the present study also suggest a possible molecular mechanism involved in TZ entry into the brain. Altered BBB expression might lead to increased TZ residue levels in the brain, which would confer neurotoxic effects often involving (a) the generation of reactive oxygen species, as shown in one of our previous studies **(Jain et al 2011)**, leading to the onset or progression of damage to normal physiological functions of different brain components, (b) the inhibition of AChE activity and (c) cognitive impairment in

the hippocampus region (Jain et al 2013). Physiologically, the BBB protects the brain from the compositional fluctuations of compounds that occur in the circulation and plays a major role in maintaining the constant environment required for normal brain function, i.e., neuronal homeostasis.

5. CONCLUSION

The present study revealed that TZ enters the brain by stimulating the expression and activity of OATP2. Furthermore, the increased residual concentration of TZ in the brain, which is strongly correlated with increased OATP2 expression, is also attributed to its decreased elimination by PGP. However, future research with the aim of analyzing the specific interaction between organophosphates and PGP in terms of conformational changes occurring during binding, either in the structure of the compound or transporter, is needed along with the implementation of additional molecular techniques and drug–receptor binding assays to distinguish different OPs as substrates or inhibitors of BBB transporters. Furthermore, understanding the nature of such specific interactions will help to identify molecular targets involved in neurotoxicity and/or neurodegeneration, thus paving the way for the design of new therapeutic strategies.

ACKNOWLEDGMENT & FUNDING

The authors acknowledge Dr. Mohit Mehndiratta, Assistant Professor, Department of Biochemistry, UCMS, for providing his kind help and support during the utilization of the real-time PCR system, which is kept under his supervision. The authors also acknowledge the support from Department of Biostatistics, UCMS, for providing support for analyzing the results statistically. One of the authors, Ms. Smita Jain, is grateful to the Council of Scientific and Industrial Research (CSIR) for providing financial support as a Senior Research Fellowship. The present work was a part of the doctoral thesis of the author (Dr Smita Jain) and has not been published (in part or full) in any other journal to date. The present study was approved by the Institutional Animal Ethics Committee, University College of Medical Sciences (University of Delhi) and Guru Teg Bahadur Hospital, as mentioned in the approval letter attached as a supplementary document.

CONFLICT OF INTEREST

The authors declare no potential conflicts of interest with respect to the research, authorship, and/or publication of this article. The present work is part of the doctoral thesis of the corresponding author and has not been published (in part or full) anywhere else.

REFERENCES

1. Agarwala, S., Chen, W. and Cook, T.J., 2004. Effect of chlorpyrifos on efflux transporter gene expression and function in Caco-2 cells. *Toxicology in Vitro*, 18, pp.403–409.
2. Bain, L.J. and LeBlanc, G.A., 1996. Interaction of structurally diverse pesticides with the human MDR1 gene product P-glycoprotein. *Toxicology and Applied Pharmacology*, 141, pp.288–298.
3. Bain, L.J., McLachlan, J.B. and LeBlanc, G.A., 1997. Structure-activity relationships for xenobiotic transport substrates and inhibitory ligands of P-glycoprotein. *Environmental Health Perspectives*, 105, pp.812–818.
4. Bartels, A.L., Willemsen, A.T., Kortekaas, R., de Jong, B.M., de Vries, R., de Klerk, O., van Oostrom, J.C., Portman, A. and Leenders, K.L., 2008. Decreased blood–brain barrier P-glycoprotein function in the progression of Parkinson's disease, PSP and MSA. *Journal of Neural Transmission*, 115, pp.1001–1009.
5. Bauer, B., Hartz, A.M., Fricker, G. and Miller, D.S., 2005. Modulation of P-glycoprotein transport function at the blood brain barrier. *Experimental Biology and Medicine (Maywood)*, 230, pp.118–127.
6. Bock, R. and Their, W., 2006. Metabolism and fate of triazophos in rats. *Pesticide Science*, 7, pp.307–314.
7. Duan, Y., Guan, N., Li, P., Li, J. and Luo, J., 2016. Monitoring and dietary exposure assessment of pesticide residues in cowpea (*Vigna unguiculata* L. Walp) in Hainan, China. *Food Control*, 59, pp.250–255.
8. Gao, B., Stieger, B., Noe, B., Fritschy, J.M. and Meier, P.J., 1999. Localization of the organic anion transporting polypeptide 2 (Oatp2) in capillary endothelium and choroid plexus epithelium of rat brain. *Journal of Histochemistry & Cytochemistry*, 47, pp.1255–1263.
9. Gottesman, M.M., 2002. Mechanism of cancer drug resistance. *Annual Review of Medicine*, 53, pp.615–627.

10. Guo, G.L., Choudhuri, S. and Klaassen, C.D., 2002. Induction profile of rat organic anion transporting polypeptide 2 (oatp2) by prototypical drug-metabolizing enzyme inducers that activate gene expression through ligand-activated transcription factor pathways. *Journal of Pharmacology and Experimental Therapeutics*, 300, pp.206–212.
11. Hagenbuch, B. & Meier, P.J., 2003. The superfamily of organic anion transporting polypeptides. *Biochimica et Biophysica Acta (BBA) - Biomembranes*, 1609(1), pp.1–18. DOI: 10.1016/S0005-2736(02)00633-8.
12. Jain, S., Banerjee, B.D., Ahmed, R.S., Arora, V.K. & Mediratta, P.K., 2013. Possible role of brain-derived neurotrophic factor and oxidative stress in Triazophos-induced cognitive impairment in rats. *Neurochemical Research*, 38(9), pp.2136–2147.
13. Jain, S., Ahmed, R.S., Arora, V.K. & Banerjee, B.D., 2011. Biochemical and histopathological studies to assess chronic toxicity of Triazophos in blood, liver and brain tissue of rats. *Pesticide Biochemistry and Physiology*, 100, pp.182–186.
14. Jain, S., Mythily, S., Ahmed, R.S., Arora, V.K. and Banerjee, B.D., 2010. Induction of oxidative stress and histopathological changes by subchronic doses of Triazophos. *Indian Journal of Biochemistry & Biophysics*, 47, pp.388–392.
15. Kumari, D. and John, S., 2019. Health risk assessment of pesticide residues in fruits and vegetables from farms and markets of Western Indian Himalayan Region. *Chemosphere*, 224, pp.162–167.
16. Lee, G., Dallas, S., Hong, M. and Bendayan, R., 2001. Drug transporters in the central nervous system: brain barriers and brain parenchyma considerations. *Pharmacological Reviews*, 53, pp.569–596.
17. Leslie, E.M., Deeley, R.G. and Cole, S.P.C., 2005. Multidrug resistance proteins: role of P-glycoprotein, MRP1, MRP2, and BCRP (ABCG2) in tissue defense. *Toxicology and Applied Pharmacology*, 204, pp.216–237.
18. Livak, K.J. and Schmittgen, T.D., 2001. Analysis of relative gene expression data using real-time quantitative PCR and the 2-ΔΔCT method. *Methods*, 25, pp.402–408.
19. Mohineesh, Raj J, Rajvanshi AC, Dogra TD, Raina A. Effect of acute exposure of triazophos on oxidative stress and histopathological alterations in liver, kidney and brain of Wistar rats. Indian J Exp Biol. 2014 Aug;52(8):814-9. PMID: 25141545.
20. Musazzi, L., Cattaneo, A., Tardito, D., Barbon, A., Gennarelli, M., Barlati, S., Racagni, G. and Popoli, M., 2009. Early raise in BDNF in hippocampus suggests induction of posttranscriptional mechanisms by antidepressants. *BMC Neuroscience*, 10, p.48.
21. Organization for Economic Co-operation and Development. (2007). Decision of the Council concerning the Adoption of Revised Test Guidelines and Guidance concerning the Mutual Acceptance of Data in the Assessment of Chemicals: Test No. 407: Repeated dose 28-day oral toxicity study in rodents. OECD Publishing. https://doi.org/10.1787/9789264070684-en
22. Pivcevic, B. and Zaja, R., 2006. Pesticides and their binary combinations as P-glycoprotein inhibitors in NIH 3T3/MDR1 cells. *Environmental Toxicology and Pharmacology*, 22, pp.268–276.
23. Ramesh M, Selvaraju SG, Poopal RK, Ren Z, Li B. Impact of continuous Triazophos exposure on Labeo rohita: Physiological, biochemical, and histological alterations and IBRv2 index assessment. Pestic Biochem Physiol. 2024 Sep;204:106043. doi: 10.1016/j.pestbp.2024.106043.
24. Rani, S., Madan, V.K. and Kathpal, T.S., 2001. Persistence and dissipation behavior of triazophos in canal water under Indian climatic conditions. *Ecotoxicology and Environmental Safety*, 50, pp.82–84.
25. Schäfer, A.M., Meyer Zu Schwabedissen, H.E. and Grube, M., 2021. Expression and function of organic anion transporting polypeptides in the human brain: physiological and pharmacological implications. *Pharmaceutics*, 13(6), p.834.
26. Schinkel, A.H., 1999. P-glycoprotein, a gatekeeper in the blood brain barrier. *Advanced Drug Delivery Reviews*, 36, pp.179–194.
27. Singh, S., Tiwari, R.K. and Pandey, R.S., 2017. Evaluation of acute toxicity of triazophos and deltamethrin and their inhibitory effect on AChE activity in *Channa punctatus*. *Toxicology Reports*, 5, pp.85–89.
28. Singh, M. and Rishi, S., 2005. Plasma acetylcholinesterase as a biomarker of triazophos neurotoxicity in young and adult rats. *Environmental Toxicology and Pharmacology*, 19, pp.471–476.

29. Sreeramulu, K., Liu, R. and Sharom, F.J., 2007. Interaction of insecticides with mammalian P-glycoprotein and their effect on its transport function. *Biochimica et Biophysica Acta (BBA) - Biomembranes*, 1768, pp.1750–1757.
30. Sueyoshi, T. and Negishi, M., 2001. Phenobarbital response elements of cytochrome P450 genes and nuclear receptors. *Annual Review of Pharmacology and Toxicology*, 41, pp.123–143.
31. Tamai, I., Nezu, J., Uchino, H., Sai, Y., Oku, A., Shimane, M. and Tsuji, A., 2000. Molecular identification and characterization of novel members of the human organic anion transporter (OATP) family. *Biochemical and Biophysical Research Communications*, 273(1), pp.251–260.
32. Volk, H., Potschka, H. and Löscher, W., 2005. Immunohistochemical localization of P-glycoprotein in rat brain and detection of its increased expression by seizures are sensitive to fixation and staining variables. *Journal of Histochemistry & Cytochemistry*, 53, pp.517–531.
33. Wang, S., Hartley, D.P., Ciccotto, S.L., Vincent, S.H., Franklin, R.B. and Kim, M.S., 2003. Induction of hepatic phase II drug metabolizing enzymes by 1,7-phenanthroline in rats is accompanied by induction of MRP3. *Drug Metabolism and Disposition*, 31, pp.773–775.
34. Wang, X., Bu, H.F., De Plaen, I.G. and Tan, X.D., 2009. Milk fat globule-EGF factor 8 mRNA expression in rat splanchnic tissues during postnatal development. *International Journal of Clinical and Experimental Medicine*, 2, pp.36–40.
35. World Health Organization (WHO) and Food and Agriculture Organization (FAO). (1985).
36. Pesticide residues in food - 1983: Toxicological evaluations (No. 644, IPCS) [Monograph] World Health Organization. (2002). *Toxicological evaluation of triazophos*. Joint FAO/WHO Meeting on Pesticide Residues.
37. Zhang, F., Riley, J. and Gant, T.W., 1996. Use of internally controlled reverse transcriptase–polymerase chain reaction for absolute quantitation of individual multidrug resistance gene transcripts in tissue samples. *Electrophoresis*, 17, pp.255–260.